

# Anthropogenic particle dispersions in topsoils of the Middle Nile Delta: a preliminary study on the contamination around industrial and commercial areas in Egypt

Atef M. Abu Khatita<sup>1,2</sup> · Helga de Wall<sup>2</sup> · Roman Koch<sup>2</sup>

Received: 22 March 2015 / Accepted: 14 September 2015 / Published online: 25 January 2016  
© Springer-Verlag Berlin Heidelberg 2015

**Abstract** Increased industrialization has adversely affected various components of the environment including soil, which is the ultimate site of settling and accumulation of fly ash. Fine respirable size particles in the atmosphere are detrimental to human health and their ultimate accumulation in the soil leads to soil pollution. In this study, these particles were identified, quantified and subjected to intensive analysis by SEM/EDX. Accordingly, the physical and chemical characteristics, the origin and the pathway of such particulates are documented for the Middle Nile Delta using the magnetic susceptibility as proxy for the industrial emissions. The average bulk density of magnetic spherules varies between  $4.4 \pm 0.7$ ,  $4.8 \pm 0.9$  and  $5.4 \pm 0.6 \text{ g/cm}^3$  for the  $>125$ , 63–125 and 36–63  $\mu\text{m}$  fractions, respectively, and consists predominantly of iron oxides with variable amounts of Ti, Si, Mn, Mg, Al, Ca, Cr and Cu. Their attached grains and adhesive materials are commonly composed of various contents of Si, Al, Fe, Ca, P, Zn, Ba and S depending on their origin. The results indicated that most surface soil samples are enhanced magnetically than the natural local background magnetic signal due to atmospherically deposited urban dust. The industrial sites are characterized by highest average magnetic susceptibility value ( $47 \times 10^{-5} \text{ m}^3\text{g}^{-1}$ ) combined with highest concentration of magnetic spherules ( $66 \text{ sph.g}^{-1}$ ). Moreover, the residential area surrounding industrial zones—particularly those located in the windblown (SE)

direction—is seriously affected by industrial dust. This study provides a database to evolve strategies for remedial measures to minimize environmental degradation.

**Keywords** Urban dust · Nile Delta · Magnetic susceptibility · Anthropogenic particles · Magnetic spherules

## Introduction

During growth of population and expansion of urbanization, especially in developing countries without formal planning, residential household areas are overlapping with industrial zones. As a result, millions of people living in close vicinity to industrial areas are facing different health diseases particularly from pollutant emission. Assessment of such pollutant emission and their distribution through the urban dust considered significance in respect to the human health impacts. Contribution of the such particulate on the human health impacts can be physically by inhalation the small sized particles (diameter  $<10 \mu\text{m}$ ) or chemically by carrying pollutants such as heavy metals or polycyclic aromatic hydrocarbons (Dockery and Pope 1994; Aunan 1996; Smith et al. 1998; Pope and Dockery 1999; Pope et al. 2002; Bernabé et al. 2005; Blaha et al. 2008; Wang et al. 2011; Rai 2013). Moreover, the surface soil is more definitive aspect for tracing such particles (Li et al. 2004; Škrbic and Đurišić-Mladenovic 2007) where the pedosphere represents archive for the input aerial deposition particulates whether of geogenic/anthropogenic origin. The accumulation of heavy metals in soils is of increasing concern due to its impacts on soil ecosystems and potential health risk as well. The urban and industrial emissions contribute with valuable amount to the

✉ Atef M. Abu Khatita  
atefabukhatita@yahoo.com

<sup>1</sup> Geology Department, Al Azhar University, Cairo, Egypt

<sup>2</sup> GeoZentrum Nordbayern, Universität Erlangen-Nürnberg, Erlangen, Germany

anthropogenic heavy metal input (Jones and Olsen 1990; Banerjee 2003; Sharma and Tripathi 2008) Since most of heavy metals are emitted and transported in form of particulates, studies about the urban dust and its particulates are important for defining the origin, dispersion and concentration of heavy metal contamination in surface environment (Banerjee 2003; Duzgoren-Aydin et al. 2006; Shinggu et al. 2007). Among that particulate matters are the magnetic particles. Magnetic particles (spherules and spheroidal particles) are of great importance because they document the influence of specific industrial activities (Lougheed 1966; Dudas and Warren 1987; Jordanova et al. 2004; Maier and Scholger 2004; Bernabé et al. 2005; Shoumkova 2006; Yang et al. 2007; Coz et al. 2009; Magiera et al. 2011; Wang et al. 2014). They can be called technogenic particles (Magiera et al. 2011; Catinon et al. 2014) and as defined by Vassilev and Vassileva (1996) they are produced as a result of softening, partial and complete melting and vitrification of coal minerals, such as clay minerals, chlorite, mica, feldspars, quartz and other fluxing minerals and phases with lower melting points. Consequently, the magnetic susceptibility of the uppermost part of the soils (topsoil) can be enhanced due to the deposition of such magnetic particles that are emitted from industrial plants. Such phenomenon can be used as a proxy to determine the pollution of surface soil by the input of magnetic particles (Hunt et al. 1984; Hay et al. 1997; Petrovský et al. 2000; Wang and Qin, 2006; Kapicka et al. 2008; Kim et al. 2009; D’Emilio et al. 2010; El Baghdadi et al. 2012; Jordanova et al. 2013; El-Hasan and Lataifeh 2013; Xia et al. 2014).

In Egypt, most of the areas consist of dry desert lands; therefore, settlements have concentrated along the banks of the Nile River and its delta where fertile soils have been formed during annual spring floods. The Nile Delta forms a triangle between Cairo and the shore line of the Mediterranean Sea (Fig. 1). Ancient settlements have now grown into big cities. Although the area of the Nile Delta represents only 2.3 % of the whole terrain of Egypt, the Nile Delta bears 46 % of the total cultivated area and accommodates approximately 45 % of inhabitants. Major cities in the central part of the Nile delta are Tanta and Kafr El Zayat, commercial and industrial spots in a region of farmland.

Obviously, more than one source is responsible for the air pollution in the study area. Industrial sources include the emission of fumes and gases (e.g., SO<sub>2</sub>, NO<sub>x</sub>, and CO<sub>2</sub>) from chimneys of chemical factories, brick kilns, especially those using diesel fuel, and petroleum refineries, in addition to the dust from phosphate fertilizer factory in Kafr El Zayat. Urban sources include car exhaust and generation of methane resulting from anaerobic decomposition of organic matter present in landfill sites. Burning of

open landfill sites can emit smoke and unpleasant gases that pollute the air. What is called the ‘Black Cloud’, resulting from the burning of fields by farmers, especially burning rice straw in the fields to avoid the spread of pests and rodents is an agricultural air pollution source. As a result, it is assumed that traces of the various components (particles, dust, and elements of solutions) are fixed to the soils in different amounts and ways. Until now, the distribution characteristics of pollutant emission in the Nile Delta have not been investigated in detail.

This study presents a first evaluation of soil pollution around Tanta and Kafr El in the Nile Delta soil, whereby the major aim is to map the polluted areas and to characterize origin and pathways of anthropogenic particles. This will be a first step towards a database to evolve strategies for remedial measures to minimize environmental degradation.

## Materials and methods

### Study area

The study area in the Middle Nile Delta is located between 30°42′ to 30°56′N and 30°42′ to 31°05′ (Fig. 1). Its topographic slope is very gentle, dipping northward, changing from about 18 m (+MSL) in the south to about 8 m (+MSL) in the north, with an average value of approximately 1.2 m/10 km. The surficial view of the study area is representative of the main cultivated lands in Egypt, including channels and drains, railways and highway networks, urban and suburban areas and industrial areas. Stratigraphically, the sedimentary sequence of the Nile Delta basin is subdivided into three sedimentary cycles (Rizzini et al. 1978; Stanley and Warne 1993; Atwia et al. 2006). The oldest cycle (Miocene) begins with clayey sediments of the *Sidi Salem Fm.* and ends with the deposition of a fluvial, littoral, and lagoonal series of the *Qawasim Fm.* and evaporites of the *Rosetta Fm.* The second cycle begins with the deposition of the sandy, basal *Abu Madi Fm.* of Lower Pliocene followed by neritic marine environment of the *Kafr El Sheikh Fm.* and ends with sediments of fluvial–deltaic and inner-neritic marine environments represented by *El Wastani and Mit Ghamr Fms.* of Pliocene–Quaternary. The third cycle (Holocene) is represented by the *Bilqas Formation* of thickness ranges from 10 to 30 m in the Middle part of the Nile Delta region (Atwia et al. 2006). *Bilqas formation* represents the uppermost exposed subaerial deltaic unit in the Nile Delta region and its valley and constitutes the most fertile agricultural alluvial agriculture soils in Egypt. The mineralogical composition of the Nile Delta alluvial soil can be arranged in the following order: quartz > plagioclase >

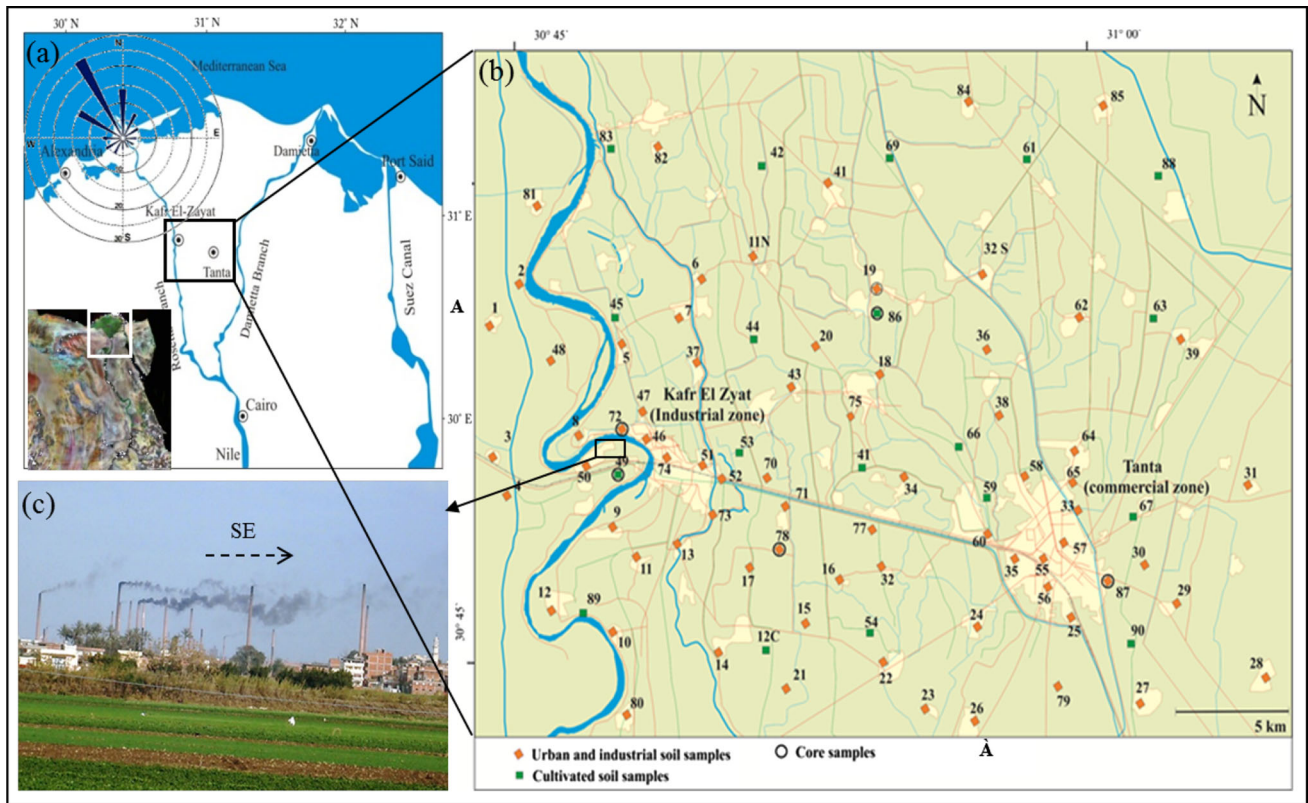


**Fig. 1** **a** Location of the study area in the Nile Delta of Egypt; **b** sampling sites around main industrial and commercial areas; **c** brick kilns at Kafr El Zyat city. The predominant direction of wind in Egypt

(Rose diagram based on data monitored by the Egyptian Meteorological Authority) is shown in the *inset*

hornblende > pyroxene > epidote > garnet > K-feldspars, and a clay size fraction predominantly consisting of smectite > kaolinite > illite (Melegy and El-Agami 2004).

The Nile Delta has a Mediterranean climate characterized by scarce rainfall with an annual average rainfall of about 37 mm<sup>3</sup>, which usually occurs from October to March. Wind speeds range from 6.9 kT in autumn to 8.3 kT in spring, but sometimes exceed this range during the year (Egyptian Meteorological Authority (EMA)). The wind direction is variable; however, the predominant direction is north–west (Fig. 1).

The Middle Nile Delta region is well known for agricultural activity over thousands of years, especially the cultivation of rice and cotton. In addition to agricultural and residential areas, this area contains the oldest and most important industrial and commercial cities in Egypt: Tanta and Kafr El Zayat. Tanta is the principal commercial centre in the Middle Nile Delta including an urban area of 33 km<sup>2</sup> with a population of 966,000 (2007). Kafr El Zayat is located directly on the right bank of the Rosetta branch of the River Nile. The urban area of Kafr El Zayat is about 17 km<sup>2</sup> with a population of 387,555. It has a long history of industrial activity, particularly in the field of chemical

and agrochemical production and this region includes the largest fertilizer, pesticide and insecticide factories in Egypt.

**Soil sampling and analysis**

Since more than one source is responsible for dispersion of the pollutants in the soil as described above, there should be differences in the enrichment of these parameters in relation to the regional differences. Therefore, the study area was differentiated into three main types, e.g., agricultural, urban (residential and commercial), and industrial sites. The anthropogenic components of the soils have been separated and physically and chemically identified.

A total of 88 representative samples (Fig. 1) of top soil (0–3 cm) have been taken from areas of different land uses (industrial, commercial, residential and cultivated sites). Each sample represents an area of about 5 × 5 m and was mixed thoroughly. Sampling close to the main motorway and railways has been avoided as much as possible. Only the uppermost 3 cm has been sampled for this study. These samples were collected using a small plastic shovel. About

0.75–1.25 kg of soil was collected from each sampling site and stored in plastic containers. Cultivated soil samples were collected from the agricultural lands that grow seasonal crops. Soil samples were collected from gardens, graves, playgrounds and parks from commercial zones and different sites near villages and residential areas. During this sampling stage we focused on the residential communities located downwind from the industrial zone to investigate the effect of industrial plants on the surroundings. Soil samples were collected from the cities of Kafr El Zayat and Tanta close to the main industrial plants. For further comparison, burnt material from pills accumulated at the foot of chimneys in industrial sites was also obtained. Moreover, to distinguish the anthropogenic input from natural background, six manual push cores ( $50 \pm 5$  cm length and 6 cm diameter) were collected from different land use sites (2 cores from industrial, 2 cores from residential and 2 cores from cultivated sites).

A total of 12 thin sections of different soil types were prepared and investigated under the polarizing microscope. The magnetic susceptibility of collected surface and downcore soil samples was determined using the kappabridge KLY-4S (AGICO, Brno) at the Geozentrum Nordbayern (GZN), Erlangen for monitoring the distribution of industrial emission in the area under investigation. The individual sample was placed in a cylindrical plastic container (ca.  $8 \text{ cm}^3$ ) and measured in low field (300 A/m). This procedure was repeated three times for each sample and the average value gives an accuracy of about 0.1 %. The kappabridge operates with a frequency of 875 Hz and a sensitivity of  $3 \times 10^{-8}$  SI. For calibration and comparison with other results, the magnetic susceptibility is divided by the sample weight (mass susceptibility  $\chi$ ), which was determined for air-dried samples before the measuring procedure.

For anthropogenic particles separation, air-dried subsamples (50 g) were wet sieved to different grain size ( $>125$ , 63–125, 36–63  $\mu\text{m}$ ) after ultrasonic desegregation. Every grain size fraction was transferred to 500-ml glass beaker. In the aqueous bath, the magnetic particles were separated from the bulk sample using a magnetic stirring bar. The wet sample with embedded magnet was lifted to magnetic plate stirrer for 3 min with stirrer rate 100–150 rpm. The magnetic bar is extracted and washed by water in cleaned ceramic plate. This step was repeated until the magnetic bar was extracted apparently without any black film (magnetic particles) attached to its both poles. Both the ceramic plate with wet magnetic particles and the remaining apparently magnetic particle-free sample were dried (40 °C) and subjected afterward to optical microscope for investigation, counting and picking up the industrial and anthropogenic magnetic and non-magnetic

particles. To evaluate this method, each run was repeated to ensure that the semiquantitative measurements can be compared between different samples without any partiality. The total numbers of magnetic spherule particles of different grain size fractions were counted into size groups of 10  $\mu\text{m}$  intervals using an eyepiece graticule, a routine described in McLean (1991).

The morphological and chemical characteristics of the selected anthropogenic particles were made at Zentrum für Werkstoffanalytik Lauf, using a LEO 1525 Gemini field emission scanning electron microscope (SEM) operating at 15 kV equipped with X-ray Dispersive Energy Spectrometry (EDX). The separated particles were coated by carbon.

The density of the various magnetic spherules occurring in different grain size fractions was determined based on their mass and volume. 10 samples were weighted for every fraction. Every sample contained 10–15 grains in the finest fraction ( $<36$ –63  $\mu\text{m}$ ), 5–10 grains in the medium grain size fraction (63–125  $\mu\text{m}$ ) and 1–3 grains in the coarse grain size fraction), using a very sensitive micro-analytical balance (Sartorius MC5). To calculate the volume, the diameter of the individual spherules was measured using a digitized optical microscope (Leica M420). Then, the density of every fraction was calculated based on the average mass and volume of the spherules. For accuracy, the density of different fractions of pure minerals quartz, apatite and magnetite was calculated. The standard deviation (SD) of these measurements lies between 7 and 17 %.

For mapping of the polluted area, two different methods have been tested: (1) tracing aerial distribution of industrial magnetic particles by semiquantitative measurements (spherules per gram) counted under the optical microscope and (2) magnetic susceptibility measurement “ $\chi$ ” ( $\text{m}^3\text{g}^{-1}$ ) of the same bulk samples. As pronounced formerly both the methods are based on the evidence that industrial and urban dust contains relatively high amounts of different grain size fractions of magnetic particles and often correlated to heavy metal concentration. The regional distribution of the amount of industrial magnetic particles is considered to reflect the distribution pattern of pollutants as a function of the wind direction in general. Contour map and 3D wire-frame maps “as approximative indicators” of semiquantitative data (spherules per gram) and magnetic susceptibility data are shown to visualize the industrial emission and its influence on neighboring areas for the Middle Nile Delta. For documentation of the natural background we have also included examples of vertical magnetic susceptibility logs from shallow downcores and the average magnetic susceptibility values of lowermost parts of the downcores are assumed to represent the natural local background magnetic signal.

## Results

### Soil characteristics from downcores

To distinguish anthropogenic input from the natural (local) background of soils (geogenic/lithogenic and pedogenic contributions; Hanesch and Scholger 2002; El Baghdadi et al. 2012), the magnetic susceptibility has been recorded in downcores to a depth of 50 cm (Fig. 2). Downcores from cultivated soils show homogeneity with massive, slightly hard, and of medium to coarse subangular blocky structure. They show an upper tillage layer which in general is about 25-cm thick but locally can become up to 40-cm thick. The lowermost parts are characterized by a thin to very thin platy layer structure. By contrast, urban and industrial soils reveal a vertical and spatial heterogeneity in their structure, at least in the upper surface layer (0–15 cm) relative to the cultivated soil. In all soil types, the upper horizons are characterized by medium-sized subangular coagulated particles and single sedimentary grains. Open cracks (0.3–0.7 mm in size) formed by drying (shrinkage cracks) and anthropogenic materials (soot, single grains, e.g., gravel, minerals and rock fragments) are common. The middle part of the downcore soils is more massive, very hard, dewatered, and has a medium-sized subangular blocky structure. The lower part is very fine grained and exhibits a fine to medium platy structure consisting of single plates of about 3–7 mm thick.

All profiles display a variability and general enhancement of magnetic susceptibility in the upper part (uppermost 30 cm) but with differences within and between the different soil types. In the lower parts (30–50 cm) the values are quite constant; the variation of the average value of magnetic susceptibility of all soil downcores is  $35 \times 10^{-5} \text{ m}^3 \text{ g}^{-1}$  (standard deviation of  $3.8 \times 10^{-5}$ ). This value can be used as an approximate value for the natural local background magnetic signal of the Nile Delta soil.

### Soil mineralogy

According to the SEM/EDX analysis, the main primary mineral components are quartz, K-feldspars and biotite with occurrence of amphiboles, pyroxenes, garnet iron oxide minerals and glauconite grains imbedded in very fine grained groundmass of high organic matter content. The urban and industrial soil samples are characterized by occurrence of grain fragments and dark particles most probably of anthropogenic sources while these components are missing in the cultivated areas. These samples contain, black spheroidal particles with different grain size scattered in a fine-grained groundmass (Fig. 3). These non-geogenic particles were separated, estimated and subjected to intensive analysis by SEM/EDX. The separated non-geogenic particles are classified and described in the following.

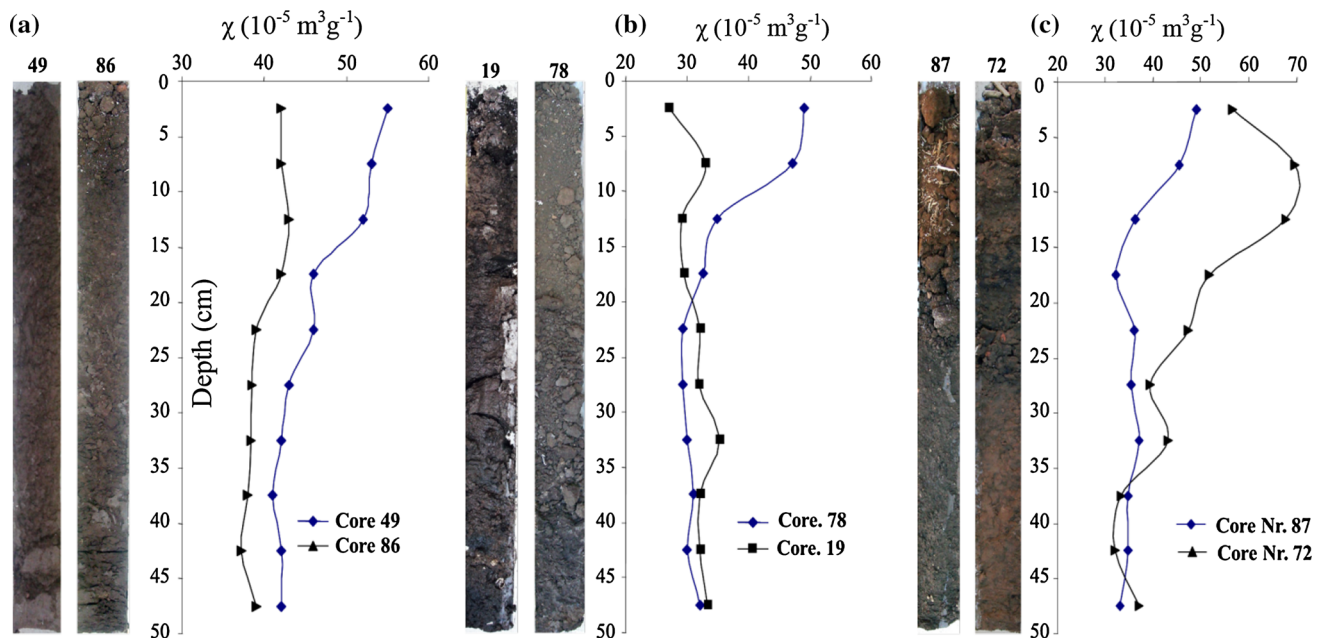
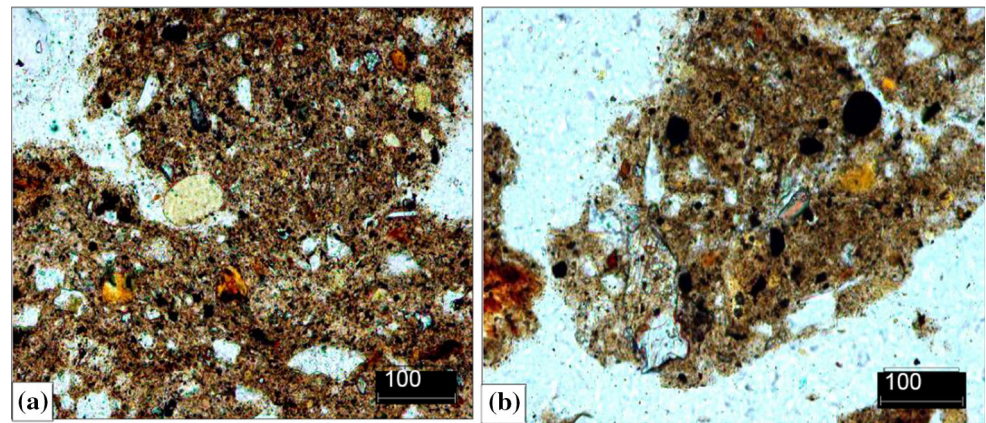


**Fig. 2** Vertical distribution of the magnetic susceptibility within the downcore soil samples of the different land use types; **a** cultivated; **b** residential and **c** industrial lands

**Fig. 3** Internal structures and particles of surface soil samples; **a** surface soil material with fine-grained, mixed porphyroskelic fabric.//Nic.; **b** black spherules of industrial source in clayey sediment.//Nic



### Morphology, chemical characteristic and origin of particles

Anthropogenic particles originating from various sources of human and industrial activities can be classified according to their magnetic characteristics (magnetic, magnetically attracted, and non-magnetic), their morphology (spherules; non-spherules) as seen under the light microscope and their chemical characteristics based on SEM/EDX analysis. Their relative abundance is compiled in Table 1, and their size distribution throughout different soil types is illustrated in Fig. 4.

Non-magnetic particles are represented by glassy, transparent to opaque spherules of various colors, by mineral and rock fragments, by soot aggregates, glass, plastic fragments, and biogenic particles. Based on chemical and morphological parameters, the non-magnetic particles can be subdivided into siliceous spherules, calcareous particles, Ca-rich particles, Ca–P-rich particles, carbonaceous particles. Furthermore few irregular fragments of different origin are seen.

*Siliceous spherules* vary from a glassy, transparent to opaque appearance, with diameters ranging from 5 to 500  $\mu\text{m}$ . They are composed predominantly of silica with varying amounts of aluminum, iron, calcium sodium, potassium, magnesium, manganese and carbon. The concentration of Al, Fe, Ca, Na, K, Mg and Mn of spherule decreases with increasing transparency. Siliceous spherules collected from cultivated areas and from both urban and industrial areas can be differentiated by size, color, transparency, surface morphology and element contents occurring together with silica (Fig. 5). In cultivated areas, siliceous spherules are transparent to semitransparent with various colors (white gray, yellow and red). They show a predominantly glassy surface and are characterized by a relatively small particle size (diameter 5–80  $\mu\text{m}$ ). The chemical characteristics as inferred from EDX analysis indicate that impurities (Fe, Ca, Na, K, Mg and Mn) do not exceed more than 17 wt% and the Fe contents range from 8 to 12 wt%.

In urban and industrial areas the siliceous spherules are commonly spheroidal, frequently opaque and characterized

**Table 1** Relative abundance of particles collected in the different surface soil types

Particle type				Soil type		
				Cultivated	Urban	Industrial
Non-magnetic particles	Siliceous	Si-rich	Sph.	xxx	x	x
			Non-sph.	x	x	xx
	Fe-bearing		Sph.	xx	xxx	xxxx
			Non-sph.	xx	xx	xxxxx
			Sph.	xxx	–	–
	Calcareous	Ca-rich	Sph.	xxx	–	–
			Non-sph.	xx	xxxxx	xxxxx
	P-bearing	Sph.	xx	xx	xxxx	
		Carbonaceous spherules	xx	xxxxx	xxxxx	
	Mineral fragments		Hal., Gyb.	Hal., Gyb., Ap., S	Hal., Gyb., Ap., S	
Magnetic particles	Spherules (cenosphere and plerospheres)		x	xxxx	xxxxx	
	Slag and iron. fragments		xx	xxx	xxxxx	

*Sph.* spherules, *Hal.* halite, *Gyp.* gypsum, *Ap.* apatite, *S.* sulfur, *x* trace, *xx* present, *xxx* common, *xxxx* abundant, *xxxxx* very abundant

**Fig. 4** Anthropogenic particle size ranges within the different soil types

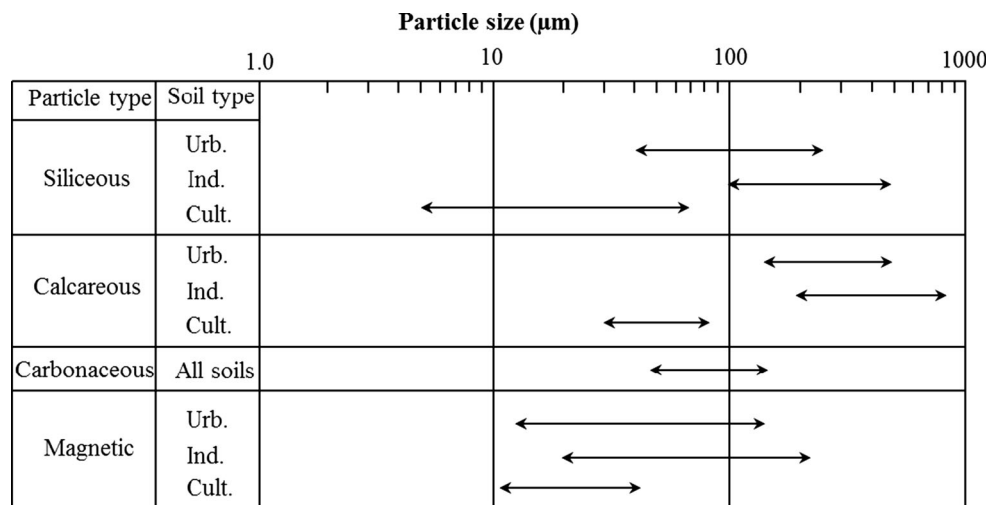
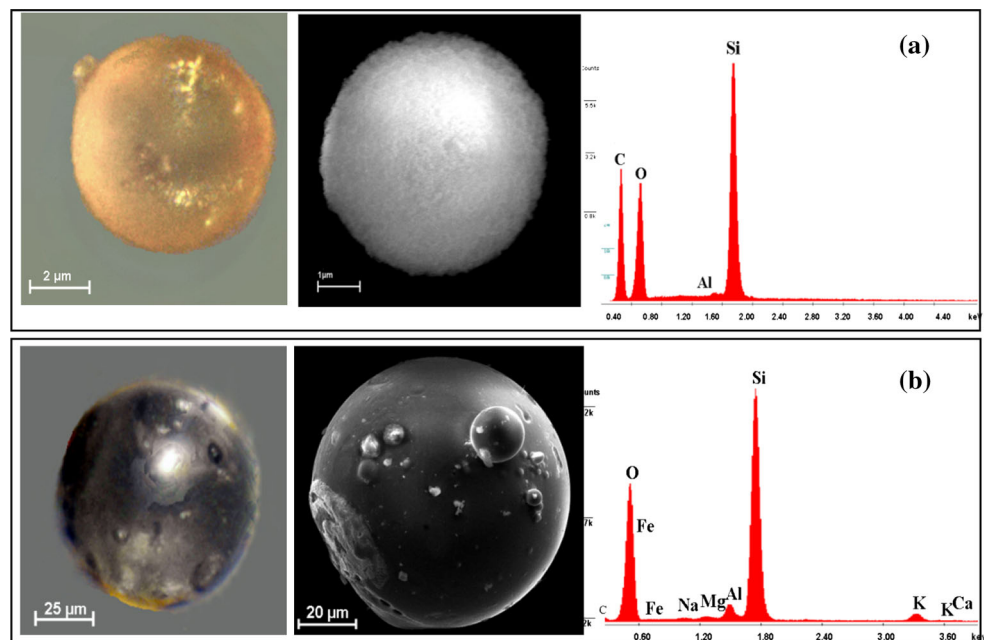


**Fig. 5** Binocular microscope and SEM photomicrographs with corresponding EDX analysis of; **a** yellow and gray and **b** transparent siliceous spherules, collected from cultivated soils

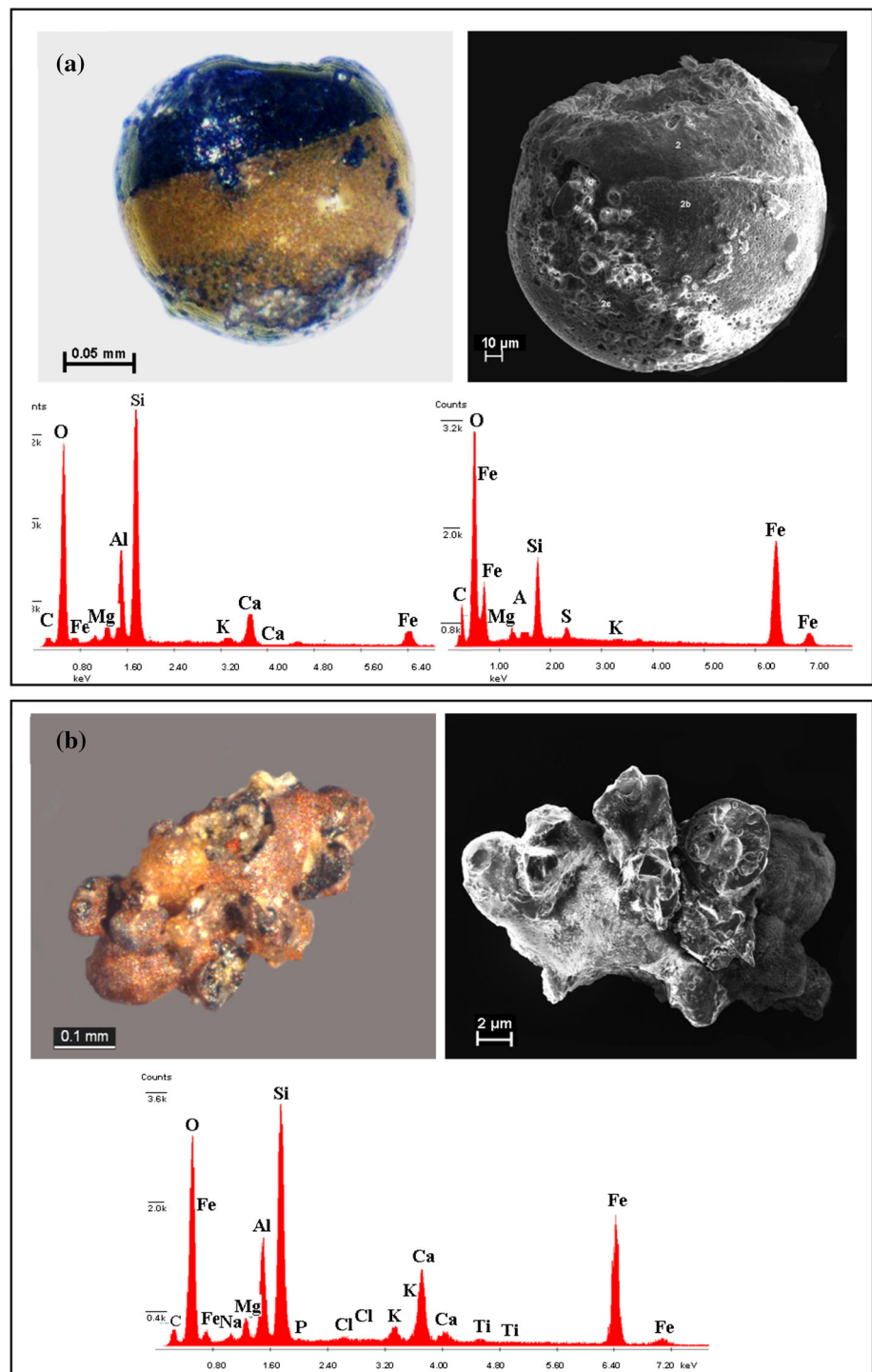


by uneven surfaces and coarser sizes (50–500 µm). The level of impurities as documented by the amounts of Fe, Ca, Na, K, Mg and Mn is relatively high (27–48 wt%). The Fe content can reach 38 wt% in cases where siliceous spherules appear to be mixed with iron-rich materials. Siliceous spherules from industrial and urban areas can be differentiated just by their mean size. In industrial areas the spherules are coarser (100 µm–0.5 mm) than in urban areas (40–250 µm). Furthermore, the most collected urban siliceous spherules were collected from windblown of industrial dust. Along with Al and Fe and other elements (Ca, Na, K, Mg and Mn) analyzed in very low amounts in siliceous spherules from cultivated areas, Cu, Zn and Ti are also found as traces in siliceous spherules from urban and industrial areas (Fig. 6).

*Calcareous particles* are particles in which oxygen and calcium make up between 73 and 97 wt% and in general contain more than 25 wt% of calcium with minor amounts of other elements (e.g., P, Mg, S, Si, and Na). These particles are further subdivided into *calcium-rich* particles (Ca content more than 37 wt%) and *Ca-P-rich* particles (phosphorus content is more than 10 wt%).

*Ca-rich particles* occur as spherules, tablets, and capsules or have a bar-like shape. They are relatively small in size (30–80 µm). The spherule-shaped particles are transparent, exhibit a yellow color and reveal a granulated surface. They are composed predominantly of Ca with minor amounts (<2.5 wt%) of P, Mg and Na. These particles were found only in cultivated soil samples (Fig. 7a). The other forms (spheroidal, tablet, capsules or bar like) of

**Fig. 6** Binocular microscope and SEM photomicrograph with corresponding EDX analysis of **a** mixed siliceous, Fe-bearing spherules collected from urban soil (SE industrial zone). The EDX analysis at the *left side* shows predominantly the siliceous yellowish part while the composition of the iron part, at the *right side*. **b** Represents clusters of spheroidal particles of siliceous and Fe-bearing spherules collected from dust piles near a brick chimney arising from brick kilns



Ca-rich particles have a pale white color and a size range of 0.8 mm–150 μm. Along with Ca, other elements (Fe, K, Mg, P and S) are present in small amounts (<5 wt%). These types of particles occur in all investigated soil types in the southeastern section of the study area. Their abundance can be ordered according to industrial > urban >> cultivated soil. In industrial areas the bar-like forms prevail and become platy and translucent with

increasing distance from the potential industrial source (Fig. 7b).

*Ca–P-rich particles* are observed in small amounts forming larger spherules. They are characterized by a white color with a shiny smooth surface and sizes range from 100 to 250 μm. They are composed predominantly of Ca and P with small amounts of K, Mg, Na, Si and Al. Under a binocular microscope, some individual spherules have



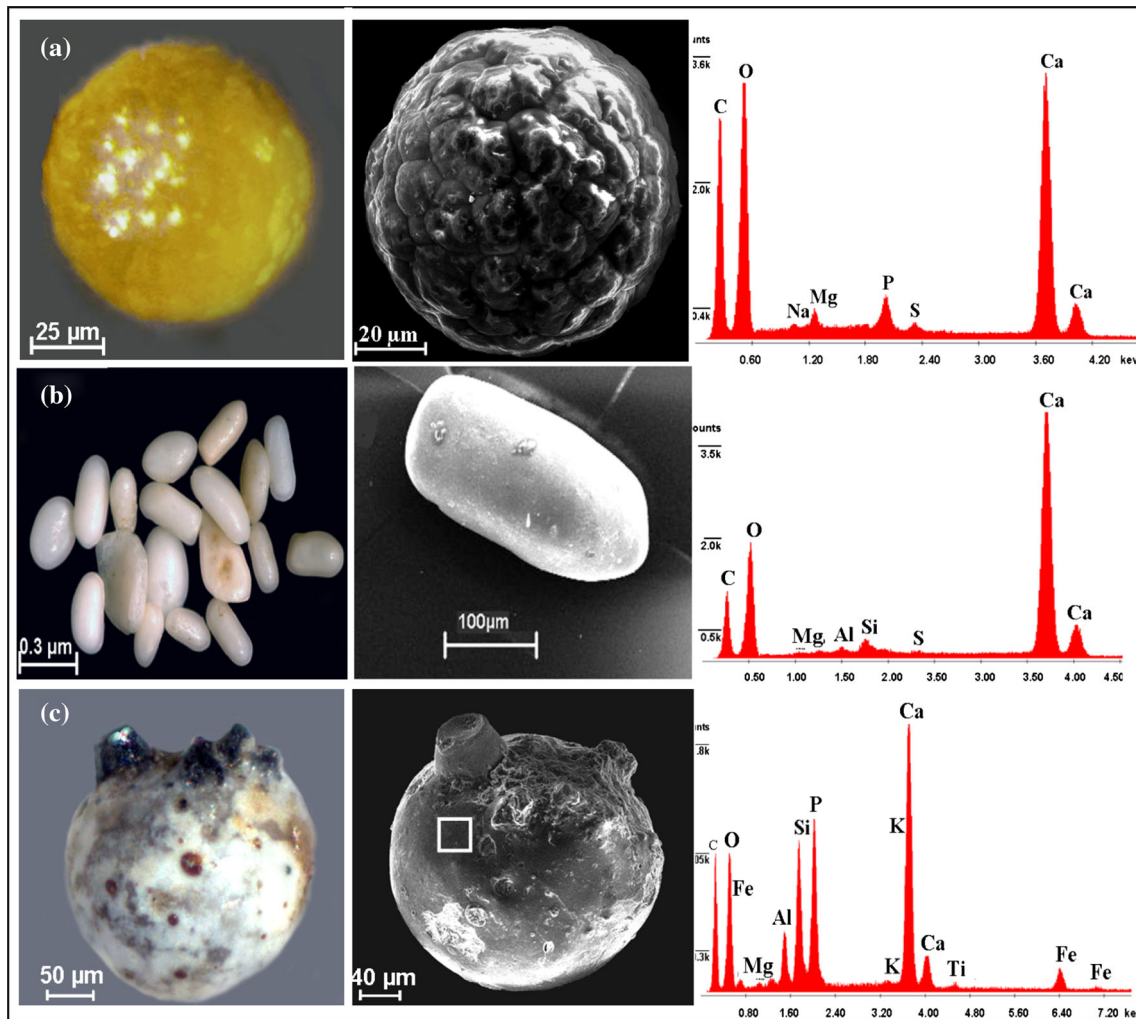


**Fig. 7** Varieties of non-magnetic anthropogenic particles collected from different soil types: binocular microscope (*left*) and SEM photomicrograph (*right*) with a corresponding EDX analysis. **a** Ca-

rich calcareous spherule collected from cultivated soil; **b** P-calcareous non-spherule particles collected from industrial soil and **c** Ca-rich calcareous particles

marbled surfaces with dark brown spots (Fig. 7c). EDX analysis reveals that these brown spots are composed of Si and Al with minor amounts of K, Mg and Na and are, therefore, interpreted as relics of clay minerals from the soil fixed to the surface of the spherules.

*Carbonaceous particles* occur in varying amounts as spherules in all the soil types analyzed. But, they are not very common in residential and cultivated areas (less than 3–6 %), whereas they are abundant (30–50 %) in high traffic sites of commercial and industrial areas. Carbonaceous particles (Fig. 8) are soft, friable and have diameters ranging from 50 to 150 μm. The surface of spherules can be smooth, rough, porous, spongiform, cellular and sometimes reveal an etched convoluted texture with a dark gray to black color. Carbonaceous spherules are composed nearly exclusively of carbon. Due to the analysis by EDX, for which the samples were coated with carbon, the carbon content of the spherules was not analyzed. The spherules

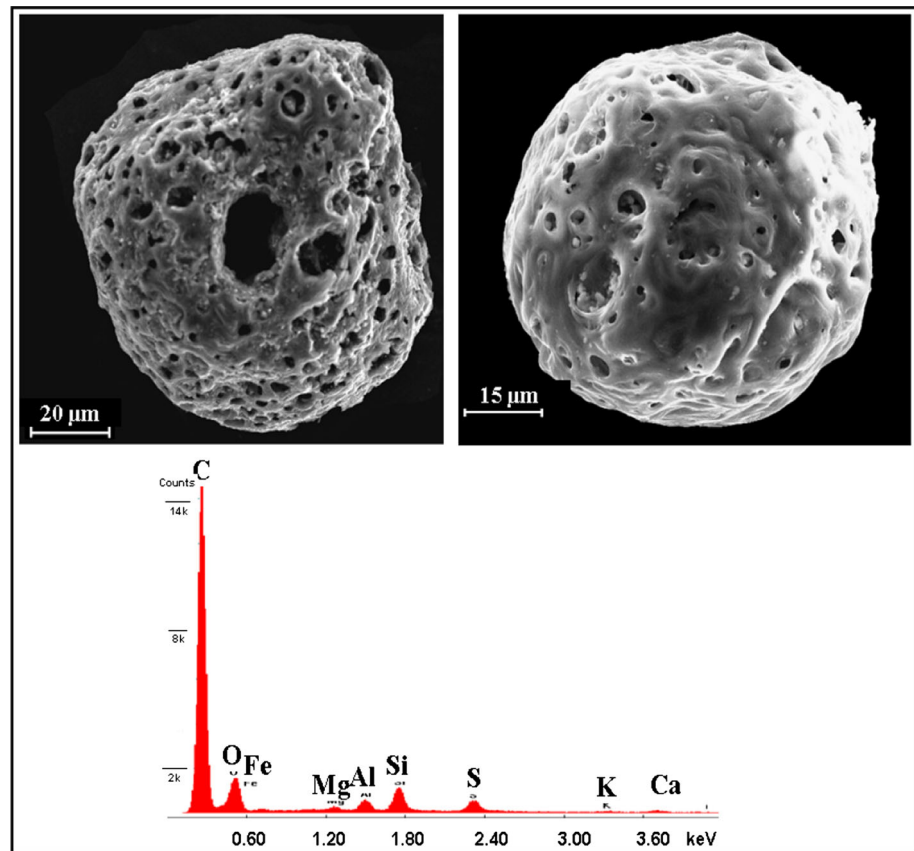
contain minor amounts of S, Si, Fe Mg, Al and sometimes Mg and Ti.

*Irregular fragments* include fragments of phosphatic rocks, limestone, and other crystalline and sedimentary rocks. Furthermore, aggregates and single grains of minerals (e.g., halite (Na–Cl rich), sulfur (mainly S), apatite (P–Ca rich), gypsum (Ca–S) and barite (Ba–S rich) as shown by SEM/EDX analysis also occur. Other fragments are glass, plastic, rubber, non-magnetic metals, building materials and paint particles, organic and biological elements (pollen grains, vegetables and animal particle grains) and soot aggregates.

### Magnetic particles

The magnetic particles represent 65–92 % of the total separated anthropogenic particles in the different studied soil types. Magnetic particles of anthropogenic origin

**Fig. 8** SEM photomicrographs with corresponding EDX analysis of carbonaceous particles collected from urban soil. These particles most likely arise from fuel–oil composition



consist predominantly of spherules; but non-spherule shapes also occur. The spherules occur as cenospheres and plerospheres. The terms *cenosphere* and *plerosphere* are used according to Fisher et al. (1976) and describe “empty” and “capsulated with smaller particles” spherules, respectively. Hollow spheres are interpreted as a result of gas escaping from plastic spherules bursting during burning processes, as documented by Vassilev and Vassileva (1996). The sizes of spherules vary between 10 and 200 µm where their size decreases with increasing distance from the industrial zone (Fig. 9). The color ranges from black, dark gray, gray to even pale brown, with a shining metallic, submetallic to dull luster (Fig. 10a). Most magnetic particles occur as single grains; others form aggregates embedded in different cement materials. Agglomerates are rare and restricted to industrial zones. Spherules and spheroidal particles are most common. They exhibit different surface structure patterns ranging from smooth, rutted, creased or a marcasitic “brain-like” (Fig. 10b) as described by Matzka (1997) to a crystalline network surface. A network of rhombic, rhomboid forms within the crystalline surface can well be recognized (Fig. 10c). The average bulk density of spherules varies from  $4.4 \pm 0.7$ ,  $4.8 \pm 0.9$  and  $5.4 \pm 0.6$  g/cm<sup>3</sup> for the >125, 63–125, 36–63 µm fractions, respectively. Within

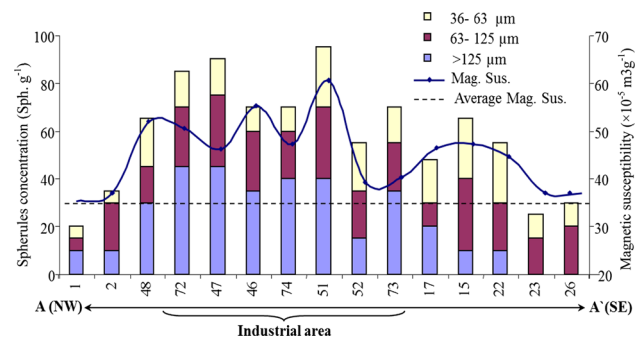
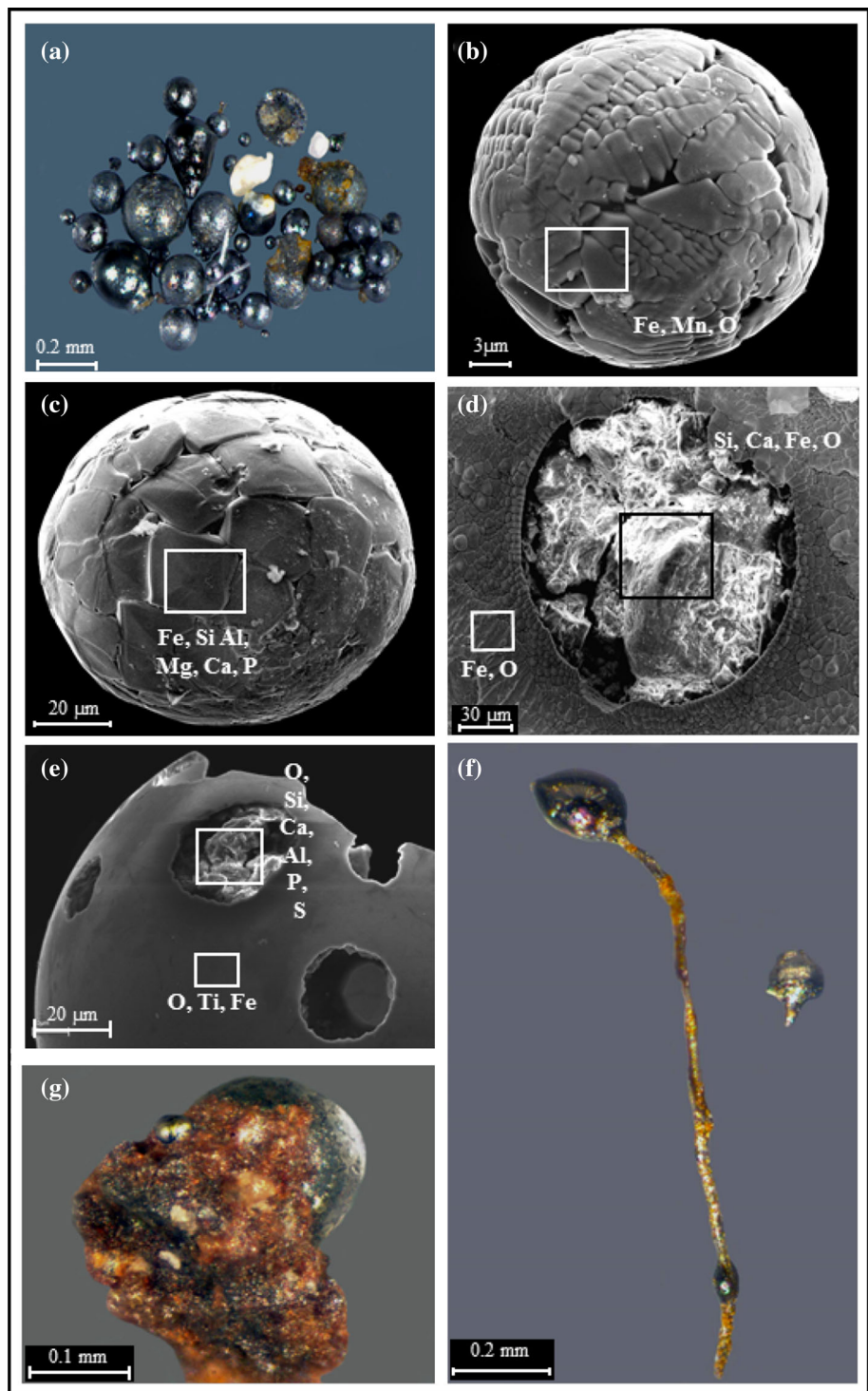


**Fig. 9** Grain size distribution of the magnetic spherules and the magnetic susceptibility (Mag. Sus., and its natural local background value) of the samples with distance to the industrial area, A–A' is cross section on the sampling location map (Fig. 1)

the same grain size fraction, shiny luster-surface Ti-bearing spherules have half the density (average 2.8 g/cm<sup>3</sup>) of the dull rustier surface spherules (average 4.9 g/cm<sup>3</sup>). No relation between the grain size of the magnetic particles and their chemical characteristics has been detected.

Small differences occur in morphological features of magnetic spherules which probably related to the aerial sorting process during transport by wind. In urban areas, magnetic spherules and their fragments commonly exhibit homogeneous cenospheres, characterized by relatively

**Fig. 10** Characteristic magnetic particles: **a** overview of magnetic spherules and nonspherical particles, **b** and **c** magnetic spherules with marcasitic and crystal pattern surface structure, respectively, **d** large pores, surface magnetic fragment filled with mixed material, **e** titanium-bearing magnetic spherules with smooth porous surface casts filled with different material, **f** nodule-type spherule connected by tails of melted material, **g** magnetic spherules of different grain sizes embedded in cement matrix; **a**, **f** and **g** are binocular while **b**, **c**, **d** and **e** are SEM photomicrographs with corresponding EDX analysis



small sizes, a black to dark gray color, and a smooth porous surface. Fragments of spherule walls are frequently observed and sometimes contain numerous surface geometric voids packed with different fine grains (Fig. 10d). The spherules with smooth surfaces commonly contain high amounts of titanium (<48 wt%) as well as iron and oxygen (Fig. 10e). Spherules with a tail-like shape, which

are coated by carbon (Fig. 10f) may indicate that they are produced by melting material of relatively high viscosity. Many magnetic spherules collected from residential samples sited within in the windblown (SE) direction of industrial zone contains attached dark red grains resembling that collected from dust piles near a brick chimney (Fig. 6).

In industrial sites, spherules have various shapes which are related to compositional variations in the burning fossil fuels used by different industrial activities. The sizes of these spherules range from 20 to 200  $\mu\text{m}$ . They vary in color from black, dark gray, gray to even pale brown, with a submetallic to dull luster. Most industrial-type spherules occur as plerospheres with a rough and mottled surface. Only minor spherules reveal a smooth surface with abundant holes. Different spheroidal shapes such as subspherical, cask-like or drop-like spherules are observed packed together with fine to very fine magnetic spherules or other mineral grains (quartz, calcite, sulfur and apatite).

SEM/EDX analysis reveal that the spherules are composed predominantly of Fe, O, and C (sometimes contain low amounts of Ti), and minor amounts of Si, Mn, Mg, Al, Ca, Cr and Cu. Commonly attached grains consist of (1) quartz (EDX; predominantly Si), (2) silicates (EDX; predominantly Al and Si, with small amounts of Ca, Mg and S), and (3) apatite (EDX; P and Ca). The common cement matrix material of a red to dark brown color (Fig. 10g) is composed predominantly of Si, Al, Fe, and Ca as well as minor amounts of P and S. Other materials commonly attached to the adhesive material of the grains are usually a pale gray color (Fig. 11) and composed predominantly of P, Ca, S, Zn, and Ba with minor amounts of Fe, Si Na and Ti.

In cultivated soil samples the abundance of spherules is very low. The magnetic particles are usually represented by disturbed, dull gray rough-surfaced cenospheres. Thin angular platy magnetic particles are mainly related to the annual plowing practices.

## Frequency and distribution of contaminants

All downcore samples collected near industrial zones (even the cultivated lands) are characterized by the distinctly enhanced magnetic susceptibility in the upper parts down to ca. 25 cm (Fig. 2) compared to the lower parts are recorded in the Kafr El Zayat industrial zone (Fig. 1b) close to the brick kilns in industrial lands (core 72: up to  $69 \times 10^{-5} \text{ m}^3 \text{ g}^{-1}$ ), even the cultivated land near the factories show strongly enhanced values (core 49:  $56 \times 10^{-5} \text{ m}^3 \text{ g}^{-1}$ ) compared to industrial areas in larger distance (core 87).

A distinct higher magnetic susceptibility in the upper part is also seen in the core from the Tanta commercial zone (up to  $49 \times 10^{-5} \text{ m}^3 \text{ g}^{-1}$ ) which is located nearby a factory of rubber, battery cases and molded products.

## Spatial distribution of contaminants

The distribution of magnetic particles is quite variable within and between the different soil types. A significant difference in average concentration for cultivated ( $0.9 \text{ sph. g}^{-1}$ ), urban ( $39 \text{ sph. g}^{-1}$ ) and industrial areas ( $66 \text{ sph. g}^{-1}$ ) is recognized (Table 2) with different levels of contamination. Surprisingly, this is not reflected in the mean magnetic susceptibility values of the respective soil types (industrial:  $48 \times 10^{-5} \text{ m}^3 \text{ g}^{-1}$  > cultivated:  $43 \times 10^{-5} \text{ m}^3 \text{ g}^{-1}$  > urban soil:  $38 \times 10^{-5} \text{ m}^3 \text{ g}^{-1}$ ) which in the cultivated soils show mean values almost as high as in the industrial areas. This failure in correlation is also

**Fig. 11** Magnetic particles embedded in matrix collected from Kafr El Zayat industrial area, (a) binocular microscope and (b) SEM photomicrograph with corresponding EDX analysis (c and d)

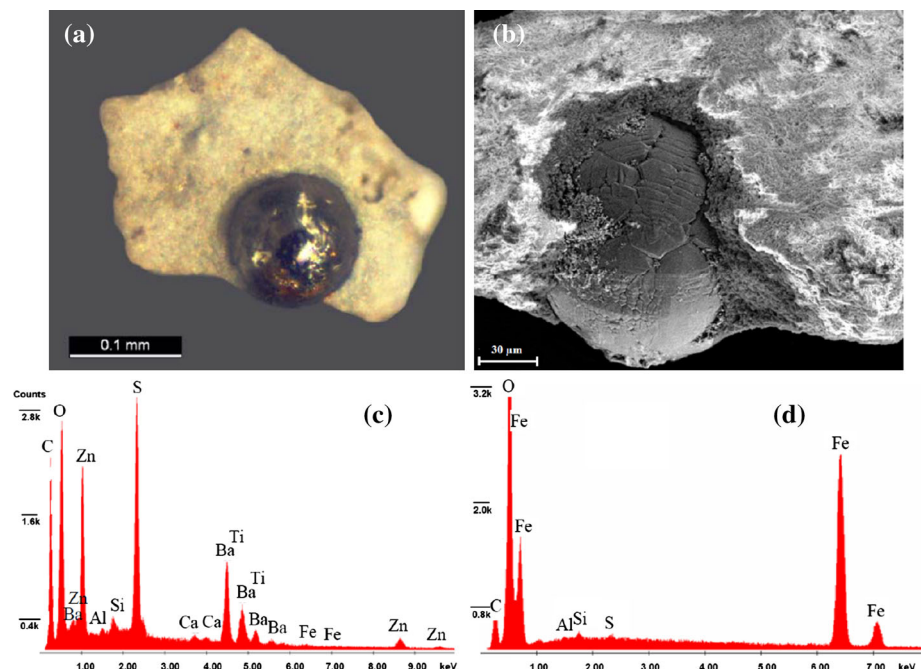


**Table 2** Magnetic susceptibility of bulk soil samples and quantitative analyses of magnetic particle concentration (Sph.g<sup>-1</sup>) and their fraction sizes in different soil types

Soil types	Urban soil			Industrial soil			Cultivated soil		
Mag. prosperities	Range	Mean	SD	Range	Mean	SD	Range	Mean	SD
Sus./g. × 10 <sup>-5</sup>	-51	38	6	39-61	48	6	28-57	43	10
(Sph.g <sup>-1</sup> )									
bulk/sample	10-80	39	18.2	30-95	65.9	21.9	0-3	0.9	1.0
36_63 mμ	5-40	14.3	8.6	0-25	12.3	7.5	0-2	0.7	0.8
63_125 mμ	0-40	15.3	7.7	10-30	22.3	7.8	0-5	0.7	1.3
>125 mμ	0-35	8.4	8.8	15-45	30	11.2	-	-	-

Given are the range of values, the average and standard deviation

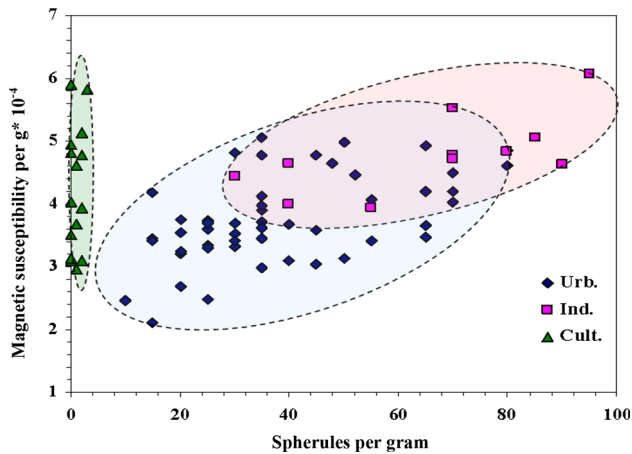


**Fig. 12** Plot of magnetic spherule per gram vs. magnetic susceptibility showing the distinctive fields of different soil samples

seen in a cross-plot of both the data sets showing the correlation for individual sites (Fig. 12).

### Discussion

Soil contaminants in the study area show a wide variability in morphology and chemical characteristics. Petrographically, identification of the non-geogenic particles is easy because of their shape and appearance which facilitates the separation from the geogenic background material. In SEM/EDX studies, siliceous spherules are well recognized among the non-magnetic anthropogenic particles and more than one source has to be considered to explain the occurrence of such particle types. In industrial zones the brick kilns are most probably the main producer of most of the siliceous spherules. This observation is supported by the analysis of samples collected from burnt material at the foot of chimneys, which contains the same siliceous spherules as found in the surface soil sediments. These samples also commonly contain individual spherules and clusters of red siliceous spherules. Siliceous particles can be produced by the reduction of SiO<sub>2</sub> in coal ash by carbon and vaporization of SiO in furnaces followed by

atmospheric oxidation and nucleation (Li and Winchester 1993; Xie et al. 2005). Siliceous spherules found in cultivated soil are produced by burning wood and straw in farmlands (Ausset et al. 1998; Olson and Jones 2001; Humphreys et al. 2003). Moreover, aluminosilicates such as clay can be transformed by agricultural fire and anthropogenic heating to sillimanite or mullite (Catinon et al. 2011; Campos-Ramos et al. 2010), forming new minerals primarily not present in the soils.

The other type of the non-magnetic anthropogenic particles which is identified in the study area is calcareous particles. The chemical characteristics and their spatial distribution indicate that they are probably derived from fertilizer additives. There is a close correlation of all these calcareous particles of various shapes and morphological features to the fertilizer factories. They can be dispersed and resuspended as particle dust around the industrial area from the pile, during the grinding processes of raw materials or during the production operations. Such calcareous particles along with other morphological properties were found near phosphatic fertilizer factories as documented in other studies (e.g., Bernabé et al. 2005; Aoun et al. 2010; Silva et al. 2010).

Carbonaceous particles compose principally of carbon with minor amounts of other elements (S, Si, Fe Mg, Al, Mg, Ti) and dispersed predominantly close to busy traffic sites. These types of spherules generally originate from fuel-oil combustion (Griffin and Goldberg 1981; Wik and Renberg 1987; Powell et al. 2002; Umbría et al. 2004; Rodríguez et al. 2009). The varying morphological features depend on the operating parameters of the combustion process as carried out by Goldstein and Siegmunce (1976).

Occurrence other fragments, e.g., halite, sulfur, apatite, gypsum and barite, most probably originated from raw materials used in different factories. It is worth mentioning that you can smell the sulfur odor at all of the sites in the Kafr el Zayat industrial area.

No doubt that the most important type among anthropogenic particles is magnetic spherules. These particles are deposited and accumulated on the surface soil layer in considerable concentration and can represent about 75 % of the total fly ash in the urban surface soil layer (Jones and

Olsen 1990). Because of the nature of their origin (e.g., industrial and power plants, metallurgy, vehicular traffic, etc.) and their large specific surface areas, these particles can be an imperative carrier for many heavy metals (Strzyszc and Magiera 1998; Karimi et al. 2011; Jordanova et al. 2014). Previous studies have shown that their concentration generally corresponds with the spatial distribution of heavy metal (Hanesch and Scholger 2002; Gautam et al. 2005; Sharma and Tripathi 2008). In the study area the magnetic spherules display great surface morphological variance. The variations in the surface morphology of the spherules are interpreted as a result of phase heterogeneity (Vassilev 1992), cooling rates (Blaha et al. 2008), variations in chemical properties (Kim et al. 2009) and/or physicochemical conditions (Shoumkova 2006; Magiera et al. 2011). Moreover, the density measurements reveal that the composition of coarser individual spherules is more porous, hollow and heterogeneous than the finer ones. The origin of different spherules can be concluded on the basis of their chemical composition, their inclusions, attached grains and cement matrix based on SEM/EDX analysis. The occurrence of higher amounts of Si, Al, Ca and Fe is most probably attributed to specific raw materials (iron-rich clay) from brick kilns and spherules produced from brick chimneys as a melting product of the iron-rich clay minerals (Vassilev 1992). By contrast, high contents of Ca, Zn, P, Mn, Ba and Fe are most probably attributed to chemical and fertilizer industries (Abu Khatita 2011). The results indicated that the aerial sorting processes play an important role in the distribution of these particles.

Except for the cultivated soil, there is a relationship between the magnetic susceptibility values and the concentration of the magnetic spherules. While for urban and industrial soils a general increase of particle concentration is also reflected in higher magnetic susceptibility values, the cultivated soils show generally low concentration and high variability in magnetic susceptibility of the individual sampling sites. Reducing the number of magnetic spherules in the cultivated surface soil samples is due to disturbance of the upper (20–30 cm) tillage arable layer. Regardless, agricultural processes and agrochemical applications are also responsible for increasing the magnetic susceptibility values in the cultivated soil than the other soil types. It has been observed that the lower parts of the soil downcores collected from cultivated lands display higher average susceptibility value ( $39 \times 10^{-5} \text{ m}^3 \text{ g}^{-1}$ ) than the other lower parts of the soil downcores collected from residential and industrial lands ( $33 \times 10^{-5} \text{ m}^3 \text{ g}^{-1}$ ). Likewise, the core (86) which is collected from the cultivated land is characterized by high susceptibility values in the upper parts than the upper parts of the core collected from adjacent residential site (core 19) in the middle part of the study

area. This most probably attributed to different deposition and migration mechanisms through the cultivated lands (Magiera et al. 2006) which reflect the effect of land use on the physical properties of the soil (Maher 1986; Kapicka et al. 2008). Such enhancing of magnetic signal in cultivated lands can attribute to fermentation processes and farming practices such as plowing, application of fertilizer and organic manure and firing in fields by farmers, especially burning rice straw in the fields. Anaerobic microbial Fe in organic-rich soil can promote higher magnetic susceptibility (Schmidt 2009) by a so-called fermentation mechanism. Microaerophilic assimilatory bacteria (magnetotactic bacteria) and anaerobic dissimilatory bacteria (GS-15 type) contribute to the magnetic properties of soils by producing magnetite (Fassbinder et al. 1990; Lovley 1991) which may oxidize to maghemite (Dearing et al. 1996). Meena et al. (2011) documented that the fertile alluvial agriculture soils usually exhibit higher paramagnetic/diamagnetic contribution and weak ferrimagnetic concentration than the surrounding soil of higher ferrimagnetic concentration values in the contaminated area. Otherwise, utilization of pesticides and fertilizer during agricultural practices (Duan et al. 2010; D'Emilio et al. 2010), burning the waste fields after the annual plow (strictly rice straw in studied area) in the presence of a reducing agent, such as organic matter, can lead to increases in magnetic susceptibility by thermal transformation of weakly magnetic iron oxides (e.g., haematite) to secondary (e.g., magnetite or maghemite), very fine (0.05–0.1  $\mu\text{m}$ ) more magnetic forms (Le Borgne 1955, 1960; Oldfield et al. 1981; Humphreys et al. 2003). The susceptibility of cultivated soil can also be enhanced by fallen and broken steel fragments from modern farming machinery (Schmidt 2009). As a result the magnetic signal of cultivated soil can affect former processes in addition to the atmospheric emissions. Moreover, the uppermost part of core 19 was characterized by low magnetic susceptibility value than the lower part of the core and lower than the assumed geogenic magnetic signal. This pattern of distribution is most probably due to admixture of the upper parts with various allochthonous grains of urban sources (e.g., quartz and concrete of fine sand grain size) of diamagnetic character.

To demonstrate the distribution of pollutant emission in the studied area, contour maps and 3D grids were established based on the spherule frequency distribution (Fig. 13) and the results of the magnetic susceptibility mapping (Fig. 14). Since the cultivated soils have very low magnetic spherule concentrations and relatively high magnetic susceptibility, the data of cultivated soil samples were excluded in the evaluation of particle distribution. The distribution pattern indicates a main anomaly located around the industrial zone (Kafr El-Zayat city) which

**Fig. 13** Contour (a) and 3D wireframe map (b) illustrating the aerial distribution of industrial magnetic particles

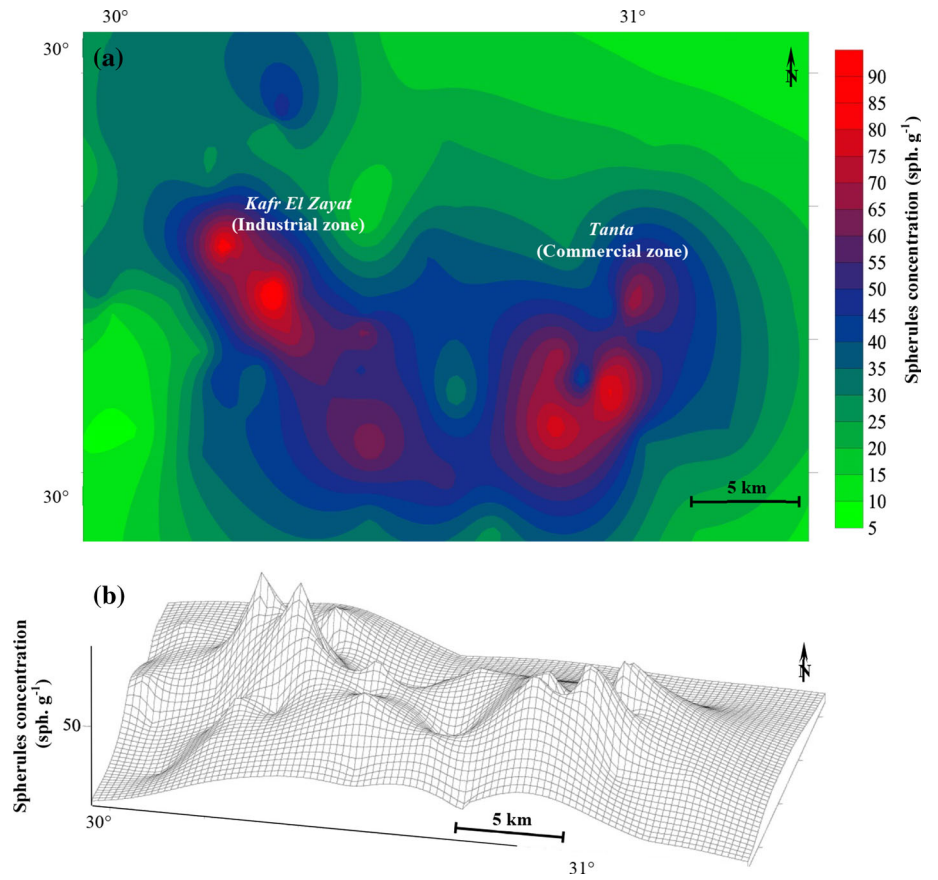
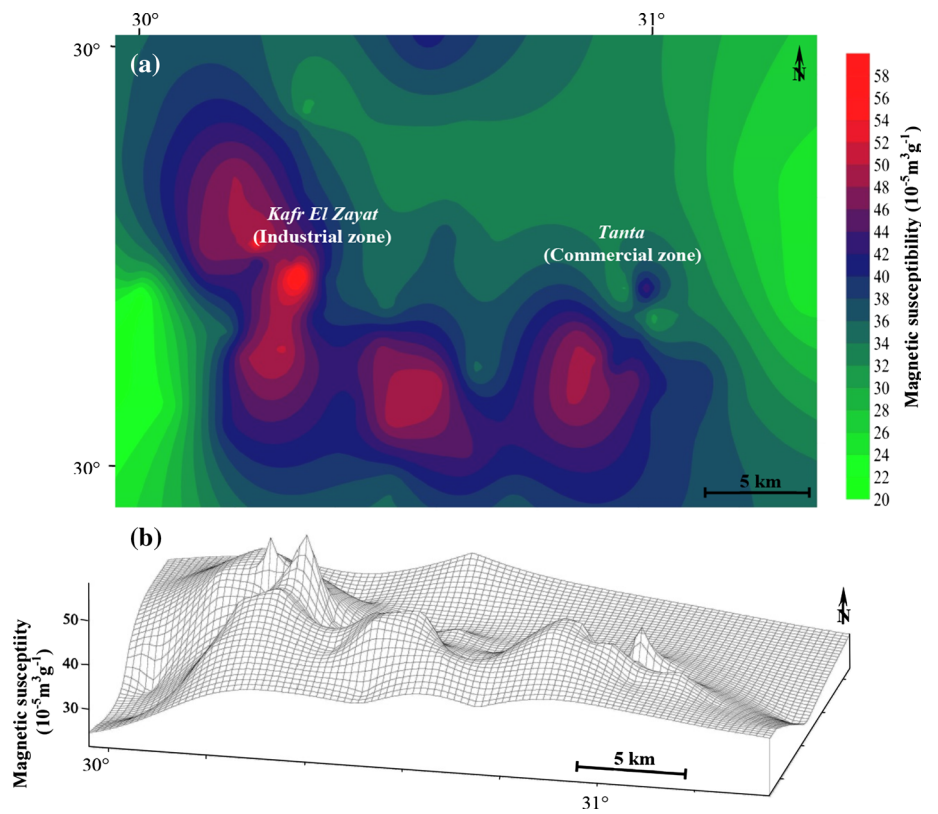


**Fig. 14** Contour map (a) and 3D wireframe map (b) illustrating the aerial distribution of the bulk magnetic susceptibility



systematically decreases in a NW to SE direction corresponding with the main wind direction. In the wind rose (according to EMA) diagram, NW represents the prevailing (26 %) wind direction of the study area beside NWW (14.8 %) and N (14 %) and other imperceptible (2.7–7.5 %) directions. Therefore, it is obvious that the amount and the size of particles correlate strongly with the main direction of the wind. The particles are blown (southeasterly) away from industrial and commercial centers in the main direction of the wind. Industrial areas are characterized by the highest concentration of unsorted spherules, whereas in surrounding urban (commercial and residential) areas, the spherules are lower in concentration and relatively uniform in size. The small discontinuity of the distribution pattern is due to the occurrence of wind-break trees. Compared with the magnetic spherules distribution pattern, a slight shifting of the magnetic susceptibility distribution pattern of the anomaly arising from the industrial zone has been occurred to the south direction. This slight shifting may be due to affecting the susceptibility by fine burned clay fragments emitted from the brick kilns and dispersed southerly by the other wind directions (particularly N) than the prevailing one. Another anomaly occurs around the commercial zone (Tanta city), which does not display a systematic decrease as documented in the industrial zone. The abundance of high chimneys (especially of brick factories which have more than 80 chimneys) in the industrial zone results in more homogeneous distribution patterns owing to undisturbed winds at a higher level. Lower chimneys in the commercial zone result in a more inhomogeneous distribution, probably due to local wind disturbances and circulation in lower wind zones induced by buildings, and trees.

The occurrence of the anthropogenic pollutant particles within the urban dust of the Nile Delta will definitely influence the air quality of such highly condensed population area (with a population density of up to 1600 inhabitants per km<sup>2</sup>). Particularly those inhalable particles pose superlative impacts on the human health. It is associated with adverse effects on respiratory system, e.g., allergic airway disease, lung cancer and increased the rate of cardiovascular mortality (Heinrich and Wichmann 2004; Brook et al. 2004; Vermeylen et al. 2005; Schwarze et al. 2006; Mills et al. 2009) and immune systems (Leonardi et al. 2000; Bateson and Schwartz 2007; Williams et al. 2011).

## Conclusions

Soil around industrial and commercial areas in the Middle Delta contaminated with different anthropogenic pollutant particles show wide variability in morphology and chemical characteristics. The magnetic phases are the major

prevailing anthropogenic particles over the investigated area, whereas, other non-magnetic particle types are less dispersed and mostly restricted to specific soil types than the others due to the land use pattern.

- Cultivated soils are characterized by siliceous spherules originating from wood and straw combustion in farmlands. Calcareous and Ca–P-bearing particles along with non-spheroidal magnetic particles arise from fertilizers and farming practices, respectively.
- Urban area sediments are characterized by the occurrence of carboniferous and magnetic spherules emitted from fuel–oil combustion due to vehicle traffic. Calcareous non-spheroidal particles arise from the deposition of industrial dust originating from the Kafr El Zayat industrial zone.
- The industrial area with the chemical and fertilizer plants was responsible for the considerable amounts of magnetic spherules along with other particles, e.g., calcareous and Ca–P-bearing particles. The brick kilns contribute large amounts of Fe-bearing siliceous spheroidal particles and magnetic spherules.

This work represents the first study on the alluvial soil of the Nile Delta (and its valley) and has documented the anthropogenic contamination of the topsoil in the Middle Nile area in the magnetic susceptibility pattern. The pollution by magnetic particles is seen in enhanced magnetic susceptibility values in the upper parts of the downcores compared to the lower parts representing the local natural background magnetic signal. Particle analysis by SEM has given evidence that magnetic particles deposited from atmospheric dust emitted from anthropogenic sources.

It is obvious from mapping of pollutants that the anthropogenic particles in the industrial zone are transported by wind in a SE direction up to a distance of 16.2 km, whereas in contrast the maximum transport distance in the commercial zone is just 4.8 km.

The occurrence of the anthropogenic pollutant particles within the urban dust of the Nile Delta will definitely influence the air quality of such highly condensed population. The concentration of such particles can be detected using environmental magnetic measurements and contaminated areas can be mapped to get constraints on the pollution pattern. However, in the context of this study only a general geochemical characterization of the anthropogenic particles, as deduced from the EDX analyses, is given. The evaluation and spatial distribution of potentially toxic elements and their accumulation in different soil types and fractions needs a more thorough geochemical characterization which is under work. However, many previous studies in heavily polluted areas all over the world have substantiated the direct link between magnetic susceptibility intensity, concentration of anthropogenic ferromagnetic



minerals and heavy metal concentration (Strzyszcz and Magiera 1998; Hanesch and Scholger 2002; Gautam et al. 2005; Sharma and Tripathi 2008) which underlines the relevance of our study for quantification of the pollution in the middle Nile Delta.

**Acknowledgments** The first author gratefully acknowledges a grant by the Egyptian mission (Higher Education Ministry) during his stay at the FAU in Germany. The staff at GZN and Dr. Jürgen Göske (Zentrum für Werkstoffanalytik, Lauf) is thanked for their assistance in laboratory work. K. Christenson is thanked for the language revision. We thank two anonymous reviewers for their constructive comments.

## References

- Abu Khatita AM (2011) Assessment of soil and Sediment contamination in the Middle Nile Delta area (Egypt); geo-environmental study using combined sedimentological, geophysical and geochemical methods. Erlangen-Nürnberg, Germany: Friedrich-Alexander University, Doctoral thesis, pp 214
- Aoun M, El Samrani AG, Lartiges BS, Kazpard V, Saad Z (2010) Releases of phosphate fertilizer industry in the surrounding environment: investigation on heavy metals and polonium-210 in soil. *J Environ Sci* 22:1387–1397
- Atwia MG, Abou-Heleika MM, El-Shishtawy AM, Sharp JMJ (2006) Hydrostratigraphy of the Central Nile Delta, Egypt, Using Geoelectric Measurements. EGS AGU EUG Joint Assem Nice Fr 5:6–11
- Aunan K (1996) Exposure-response functions for health effects of air pollutants based on epidemiological findings. *Risk Anal* 16:693–709
- Ausset P, Bannery F, DelMonte M, Lefevre RA (1998) Recording of pre-industrial atmospheric environment by ancient crusts on stone monuments. *Atmos Environ* 32:2859–2863
- Banerjee ADK (2003) Heavy metal levels and solid phase speciation in street dusts of Delhi, India. *Environ Pollut* 123:95–105
- Bateson TF, Schwartz J (2007) Children's response to air pollutants. *J Toxicol Env Health* 71:238–243
- Bernabé JM, Carretero MI, Galan E (2005) Minerology and origin of atmospheric particles in the industrial area of Huelva (SWSpain). *Atmos Environ* 39:777–778
- Blaha U, Sapkota B, Appel E, Stanjek H (2008) Micro-scale grain-size analysis and magnetic properties of coal-fired power plant fly ash and its relevance for environmental magnetic pollution studies. *Atmos Environ* 42:8359–8370
- Brook RD, Franklin B, Cascio W, Hong Y, Howard G (2004) Air pollution and cardiovascular disease: a statement for healthcare professionals from the Expert Panel on Population and Prevention Science of the American Heart Association. *Circulation* 109:2655–2671
- Campos-Ramos A, Piña AA, Querol X, Alastuey A (2010) Methodology for the characterization and identification by SEM-EDS of atmospheric particles from different pollutions emission. In: Méndez-Vilas A, Díaz J (eds) *Microscopy: Science, Technology, Applications and Education*. Formatex Research Center, pp 323–339
- Catinon M, Ayrault S, Spadini L, Boudouma O, Asta L, Tissut M, Ravanel P (2011) Tree bark suber-included particles: a long-term accumulation site for elements of atmospheric origin. *Atmos Environ* 45:1102–1109
- Catinon M, Ayrault S, Boudouma O (2014) Isolation of technogenic magnetic particles. *Sci Total Environ* 475:39–47
- Coz E, Gómez-Moreno FJ, Pujadas M, Casuccio GS, Lersch TL, Artiñano B (2009) Individual particle characteristics of North African dust under different long range transport scenarios. *Atmos Environ* 43:1850–1863
- D'Emilio M, Caggiano R, Coppola R, Macchiato M, Macchiato M (2010) Magnetic susceptibility measurements as proxy method to monitor soil pollution: the case study of S Nicola di Melfi. *Environ Monit Assess* 169:619–630
- Dearing JA, Hay KL, Baban SMJ, Huddleston AS, Wellington EMH, Loveland PJ (1996) Magnetic susceptibility of soil: an evaluation of conflicting theories using a national data set. *Geophys J Int* 127:728–773
- Dockery DW, Pope CA III (1994) Acute respiratory effects of particulate air pollution. *Annu Rev Public Health* 15:107–132
- Duan XM, Hu SY, Yan H, Blaha U, Roesler W, Appel E, Sun W (2010) Relationship between magnetic parameters and heavy element contents of arable soil around Meishan steel mill, Nanjing. *Sci China Earth Sci* 53:411–418
- Dudas MJ, Warren CJ (1987) Submicroscopic model of fly ash particles. *Geoderma* 40:101–114
- Duzgoren-Aydin NS, Wong CSC, Aydin A, Song Z, You M, Li XD (2006) Heavy metal contamination and distribution in the urban environment of Guangzhou, SE China. *Environ Geochem Health* 28:375–391
- El Baghdadi M, Barakat A, Sajieddine M, Nadem S (2012) Heavy metal pollution and soil magnetic susceptibility in urban soil of BeniMellal City (Morocco). *Environ Earth Sci* 66:141–155
- El-Hasan T, Lataifeh M (2013) Field and dual magnetic susceptibility proxies for heavy metal pollution assessment in the urban soil of Al-Karak City, South Jordan. *Environ Earth Sci* 69:2299–2310
- Fassbinder JWE, Stanjek H, Vali H (1990) Occurrence of magnetic bacteria in soil
- Fisher GL, Chang DPY, Brummer G (1976) Fly ash collected from electrostatic precipitators: microcrystalline structures and the mystery of the spheres. *Science* 192:553–555
- Gautam P, Blaha U, Appel E (2005) Magnetic susceptibility of dust loaded leaves as a proxy of traffic related heavy metal pollution in Kathmandu city Nepal. *Atmos Environ* 39:2201–2221
- Goldstein HL, Siegmund CW (1976) Influence of heavy oil composition and boiler combustion conditions on particulate emissions. *Environ Sci Technol* 10:1109–1114
- Griffin JJ, Goldberg ED (1981) Sphericity as a characteristic of solids from fossil fuel burning in a Lake Michigan sediment. *Geochim Cosmochim Acta* 45:763–769
- Hanesch M, Scholger R (2002) Mapping of heavy metal loadings in soils by means of magnetic susceptibility measurements. *Environ Geol* 42:857–870
- Hay KL, Dearing JA, Baban SMJ, Loveland P (1997) A preliminary attempt to identify atmospherically derived pollution particles in English topsoils from magnetic susceptibility measurements. *Phys Chem Earth* 22:207–210
- Heinrich J, Wichmann HE (2004) Traffic related pollutants in Europe and their effect on allergic disease. *Curr Opin Allergy Clin* 4:341–348
- Humphreys GS, Shakesby RA, Doerr SH, Blake WH, Wallbrink P, Hart DM (2003) Some effects of fire on the regolith. In: Roach IC (ed) *Advances in regolith*. CRC LEME Symposium, pp 216–220
- Hunt A, Jones J, Oldfield F (1984) Magnetic measurements and heavy metals in atmospheric particulates of anthropogenic origin. *Sci Total Environ* 33:129–139
- Jones RL, Olsen KR (1990) Fly ash use as a time marker in sedimentation studies. *Soil Sci Soc Am J* 54:855–859
- Jordanova D, Hoffmann V, Fehr KT (2004) Mineral magnetic characterization of anthropogenic magnetic phase in the Danube river sediments (Bulgarian part). *Earth Planet Sci Lett* 221:71–89

- Jordanova D, Goddu SR, Kotsev T, Jordanova N (2013) Industrial contamination of alluvial soils near Fe–Pb mining site revealed by magnetic and geochemical studies. *Geoderma* 192:237–248
- Jordanova D, Jordanova N, Petrov P (2014) Magnetic susceptibility of road deposited sediments at a national scale-Relation to population size and urban pollution. *Environ Pollut* 189:239–251
- Kapicka A, Petrovsky E, Fialova H, Podrazsky X, Dvorak I (2008) High resolution mapping of anthropogenic pollution in the Giant Mountains National Park using soil magnetometry. *Stud Geophys Geod* 52:271–284
- Karimi R, Ayoubi S, Jalalian A, Sheikh-Hosseini AR, Afyuni M (2011) Relationships between magnetic susceptibility and heavy metals in urban topsoils in the arid region of Isfahan, central Iran. *J Appl Geophys* 74:1–7
- Kim W, Doh SJ, Yu Y (2009) Anthropogenic contribution of magnetic particulates in urban roadside dust. *Atmos Environ* 43:3137–3144
- Le Borgne E (1955) Susceptibilité magnétique anormale du sol superficiel. *Ann Geophys* 11:399–419
- Le Borgne E (1960) Influence du feu sur les propriétés magnétiques du sol et sur celles du schiste et du granit. *Ann Geophys* 16:159–195
- Leonardi GS, Houthuijs D, Steerenberg PA, Fletcher T, Armstrong B, Antova T, Lochman I, Lochmanova A, Rudnai P, Erdei E, Musial J, Jazwicz-Kanyon B, Niciu EM, Durbaca S, Fabianova E, Koppova K, Lebrete E, Brunekreef B, van Loveren H (2000) Immune biomarkers in relation to exposure to particulate matter: a cross-sectional survey in 17 cities of central Europe. *Inhal Toxicol* 12:1–14
- Li SM, Winchester JW (1993) Aerosol silicon and associated elements in the Arctic high and mid-troposphere. *Atmos Environ* 27:2907–2912
- Li X, Lee SL, Wong SC, Shi W, Thornton I (2004) The study of metal contamination in urban soils of Hong Kong using a GIS-based approach. *Environ Pollut* 129:113–124
- Lougheed MS (1966) A classification of extraterrestrial spherules found in sedimentary rocks and till. *Ohio J Sci* 66:274–283
- Lovley DR (1991) Magnetite formation during microbial dissimilatory iron reduction, in Frankel RB and Blakemore RP (eds); *Iron Biominerals*. Plenum press, New York 151–166
- Magiera T, Strzyszc Z, kapicka A, Petrovsky E, MAGPROX-Team (2006) Discrimination of lithogenic and anthropogenic influences on topsoil magnetic susceptibility in Central Europe. *Geoderma* 130:299–311
- Magiera T, Jablonska M, Strzyszc Z, Rachwal M (2011) Morphological and mineralogical forms of technogenic magnetic particles in industrial dust. *Atmos Environ* 45:4281–4290
- Maher BA (1986) Characterization of soils by mineral magnetic measurements. *Phys Earth Planet Inter* 42:76–92
- Maier G, Scholger R (2004) Demonstration of connection between pollutant dispersal and atmospheric boundary layers by use of magnetic susceptibility mapping, St. Jacob (Austria). *Phys Chem Earth* 2:997–1009
- Matzka J (1997) Magnetische, elektronenmikroskopische und lichtmikroskopische Untersuchungen an Staeben und Aschen sowie an einzelnen Aschepartikeln. Diploma thesis, University Munich, Germany
- McLean D (1991) Magnetic spherules in recent lake sediments. *Hydrobiologia* 214:91–97
- Meena NK, Maiti S, Shrivastava A (2011) Discrimination between anthropogenic (pollution) and lithogenic magnetic fraction in urban soils (Delhi, India) using environmental magnetism. *J Appl Geophys* 73:121–129
- Melegy A, El-Agami NL (2004) Factors controlling the chemistry and mineralogy of selected soil types of Czech Republic and Egypt. *Bull Geosci* 79:71–79
- Mills NL, Donaldson K, Hadoke PW, Boon NA, MacNee W, Cassee FR, Sandstrom T, Blomberg A, Newby DE (2009) Adverse cardiovascular effects of air pollution. *Nat Clin Pract Card* 6:36–44
- Oldfield F, Thompson R, Dickson DPE (1981) Artificial magnetic enhancement of stream bedload: a hydrological application of superparamagnetism. *Phys Earth Planet Inter* 26:107–124
- Olson KR, Jones RL (2001) Use of fly ash as time marker in soil erosion and sedimentation studies in “Sustaining the global farm”. *Soil Conserv. Org Meeting Purdue Univ* 1059–1061
- Petrovský E, Kapicka A, Jordanoa N, Knob M, Hoffmann V (2000) Lowfield magnetic susceptibility: a proxy method of estimating increased pollution of different environmental systems. *Environ Geol* 39:312–318
- Pope CAIII, Dockery DW (1999) Epidemiology of particle effects. In: Holgate ST, Samet JM, Koren HS, Maynard RL (eds) *Air pollution and health*. Academic Press, New York, pp 673–705
- Pope C, Burnett R, Thun M, Calle E, Krewski D, Ito K, Thurston G (2002) Lung cancer, cardiopulmonary mortality and long-term exposure to fine particulate air pollution. *JAMA* 287:1132–1141
- Powell JW, Dhunt A, Abraham JL (2002) Anthropogenic vanadium-chromium-iron and cerium-lanthanum-iron particles in settled urban house dust: cCSEM identification and analysis. *Water Air Soil Poll* 135:207–217
- Rai PK (2013) Environmental magnetic studies of particulates with special reference to biomagnetic monitoring using roadside plant leaves. *Atmos Environ* 72:113–129
- Rizzini A, Vessani F, Coccetta V, Milad G (1978) Stratigraphy and sedimentation of a neogene-quaternary section in the Nile Delta Area (A.R.E.). *Mar Geol* 27:327–348
- Rodríguez I, Galí S, Marcos C (2009) Atmospheric inorganic aerosol of a non-industrial city in the centre of an industrial region of the North of Spain, and its possible influence on the climate on a regional scale. *Environ Geol* 56:1551–1561
- Schmidt A (2009) Electrical and magnetic methods in archaeological prospection. In: Campana S, Piro S (eds) *Seeing the unseen. Geophysics and landscape archaeology*. Taylor and Francis Group, London, pp 67–81
- Schwarze PE, Øvrevik J, Lag M, Refsnes M, Nafstad P, Hetland RB, Dybing E (2006) Particulate matter properties and health effects: consistency of epidemiological and toxicological studies. *Hum Exp Toxicol* 25:559–579
- Sharma AP, Tripathi BD (2008) Magnetic mapping of fly ash pollution and heavy metals from soil samples around a point source in a dry tropical environment. *Environ Monit Assess* 138:31–39
- Shinggu DY, Ogugbuaja V, Barminas J, Toma I (2007) Analysis of street dust for heavy metal pollutants in Mubi, Adamawa State, Nigeria. *Int J Phys Sci* 2:290–293
- Shoumkova AS (2006) Physico-chemical characterization and magnetic separation of coal fly ashes from “VARNA”, BOBOV DOL” and “MARITZA-ISTOKI” power plants, bulgariai-physico chemical characteristics. *J Univ Chem Technol Met* 41:175–180
- Silva LFO, Hower JC, Izquierdo M, Querol X (2010) Complex nanominerals and ultrafine particles assemblages in phosphogypsum of the fertilizer industry and implications on human exposure. *Sci Total Environ* 408:5117–5122
- Škrbić B, Đurišić-Mladenović N (2007) Principal component analysis for soil contamination with organochlorine compounds. *Chemosphere* 68:2144–2152
- Smith KR, Veranth JM, Lighty JS, Aust AE (1998) Mobilization of iron from coal fly ash was dependent upon the particle size and the source of coal. *Chem Res Toxicol* 11:1494–1500
- Stanley DJ, Warne AG (1993) Nile Delta: recent geological evolution and human impact. *Science* 260:628–634

- Strzyszcz Z, Magiera T (1998) Magnetic susceptibility and heavy metals contamination in soils of southern Poland. *Phys Chem Earth* 23:1127–1131
- Umbria A, Galán MJ, Muñoz MJ, Martín M (2004) Characterization of atmospheric particles: analysis of particles in the Campo de Gibraltar. *Atmosfera* 17:191–206
- Vassilev S (1992) Phase mineralogy studies of solid waste products from coal burning at some Bulgarian thermoelectric power plants. *Fuel* 71:625–633
- Vassilev S, Vassileva C (1996) Mineralogy of combustion wastes from coal-fired power stations. *Fuel Process Technol* 47:261–280
- Vermynen J, Nemmar A, Nemery B, Hoylaerts MF (2005) Ambient air pollution and acute myocardial infarction. *J Thromb Haemost* 3:1955–1961
- Wang XS, Qin Y (2006) Magnetic properties of urban top soils and correlation with heavy metals: case study from the city of Xuzhou, China. *Environ Geol* 49:897–903
- Wang W, Huang MJ, Kang Y, Wang HS, Leung AOW, Cheung KC, Wong MH (2011) Polycyclic aromatic hydrocarbons (PAHs) in urban surface dust of Guangzhou, China: status, sources and human health risk assessment. *Sci Total Environ* 409:4519–4527
- Wang B, Xia DS, Yu Y, Jia J, Xu SJ (2014) Detection and differentiation of pollution in urban surface soils using magnetic properties in arid and semi-arid regions of northwestern China. *Environ Pollut* 184:335–346
- Wik M, Renberg I (1987) Distribution in forest soils of carbonaceous particles from fossil fuel combustion. *Water Air Soil Pollut* 33:127–129
- Williams L, Ulrich CM, Larson T et al (2011) Fine particulate matter (PM<sub>2.5</sub>) air pollution and immune status among women in the Seattle area. *Arch Environ Occup Health* 66:155–165
- Xia D, Wang B, Yu Y, Jia J, Nie Y, Wang X, Xu S (2014) Combination of magnetic parameters and heavy metals to discriminate soil-contamination sources in Yinchuan—a typical oasis city of Northwestern China. *Sci Total Environ* 485:83–92
- Xie RK, Seip HM, Leinum JR, Winje T, Xiao JS (2005) Chemical characterization of individual particles (PM<sub>10</sub>) from ambient air in Guiyang city, China. *Sci Total Environ* 343:261–272
- Yang T, Liu QS, Chan LS, Liu ZD (2007) Magnetic signature of heavy metals pollution of sediments: case study from the East Lake in Wuhan, China. *Environ Geol* 52:1639–1650